

# Effect of substrate temperature on microstructure and optical properties of nanocrystalline alumina thin films

G. Balakrishnan<sup>a,\*</sup>, S. Tripura Sundari<sup>b</sup>, R. Ramaseshan<sup>b</sup>, R. Thirumurugesan<sup>c</sup>, E. Mohandas<sup>c</sup>,  
D. Sastikumar<sup>d</sup>, P. Kuppusami<sup>e</sup>, T.G. Kim<sup>f</sup>, J.I. Song<sup>a,\*</sup>

<sup>a</sup>Department of Mechanical Engineering, Changwon National University, Changwon 641773, South Korea

<sup>b</sup>Surface and Nanoscience Division, Indira Gandhi Centre for Atomic Research, Kalpakkam 603102, India

<sup>c</sup>Materials Synthesis and Structural Characterization Division, Physical Metallurgy Group, Indira Gandhi Centre for Atomic Research, Kalpakkam 603102, India

<sup>d</sup>Department of Physics, National Institute of Technology, Tiruchirappalli 620015, India

<sup>e</sup>Centre for Nanoscience and Nanotechnology, Sathyabama University, Chennai 600119, India

<sup>f</sup>Department of Nanomechatronics Engineering, Pusan National University, Miryang-si 627706, South Korea

Received 15 March 2013; received in revised form 11 April 2013; accepted 26 April 2013

Available online 21 May 2013

## Abstract

Aluminum oxide ( $\text{Al}_2\text{O}_3$ ) thin films were deposited on silicon (100) and quartz substrates by pulsed laser deposition (PLD) at an optimized oxygen partial pressure of  $3.0 \times 10^{-3}$  mbar in the substrate temperatures range 300–973 K. The films were characterized by X-ray diffraction, transmission electron microscopy, atomic force microscopy, spectroscopic ellipsometry, UV–visible spectroscopy and nanoindentation. The X-ray diffraction studies showed that the films deposited at low substrate temperatures (300–673 K) were amorphous  $\text{Al}_2\text{O}_3$ , whereas those deposited at higher temperatures ( $\geq 773$  K) were polycrystalline cubic  $\gamma$ - $\text{Al}_2\text{O}_3$ . The transmission electron microscopy studies of the film prepared at 673 K, showed diffuse ring pattern indicating the amorphous nature of  $\text{Al}_2\text{O}_3$ . The surface morphology of the films was examined by atomic force microscopy showing dense and uniform nanostructures with increased surface roughness from 0.3 to 2.3 nm with increasing substrate temperature. The optical studies were carried out by ellipsometry in the energy range 1.5–5.5 eV and revealed that the refractive index increased from 1.69 to 1.75 ( $\lambda = 632.8$  nm) with increasing substrate temperature. The UV–visible spectroscopy analysis indicated higher transmittance ( $> 80\%$ ) for all the films. Nanoindentation studies revealed the hardness values of 20.8 and 24.7 GPa for the films prepared at 300 K and 973 K respectively.

© 2013 Elsevier Ltd and Techna Group S.r.l. All rights reserved.

**Keywords:** C. Optical properties; Thin films; Alumina; Pulsed laser deposition; X-ray diffraction

## 1. Introduction

Aluminum oxide ( $\text{Al}_2\text{O}_3$ ) thin films possess the excellent properties such as high melting point, high hardness, medium refractive index, high transparency, low absorption, wide bandgap, high thermal conductivity, low electrical conductivity, high radiation resistance, high corrosion resistance with good chemical and thermal stability [1–3]. Hence, the  $\text{Al}_2\text{O}_3$  thin films are used as buffer layer for silicon-on insulator

devices, gate insulator for metal-oxide-semiconductor devices, metal-nitride-oxide-semiconductor and complementary metal-oxide-semiconductor devices [4–8].  $\text{Al}_2\text{O}_3$  thin films are used in anti-reflection coatings, water repellent coatings, organic light emitting devices and improving the adhesion of bioactive glasses and hydroxyapatite coatings for medical implants [9–14]. They also find many important applications in optoelectronics, wear and corrosion resistant coatings for cutting tools, oxygen permeation barrier coatings for turbine blades, hydrogen permeation barrier coatings for nuclear fusion reactors, bioceramic, catalysis, and sensors [15–18]. The surface properties of various materials such as glasses, metals, bioceramics and polymers can be modified using  $\text{Al}_2\text{O}_3$

\*Corresponding authors. Tel.: +82 552133606; fax: +82 552675142.

E-mail addresses: [jsong@changwon.ac.kr](mailto:jsong@changwon.ac.kr) (J.I. Song),  
[bala\\_physics76@gmail.com](mailto:bala_physics76@gmail.com) (G. Balakrishnan).

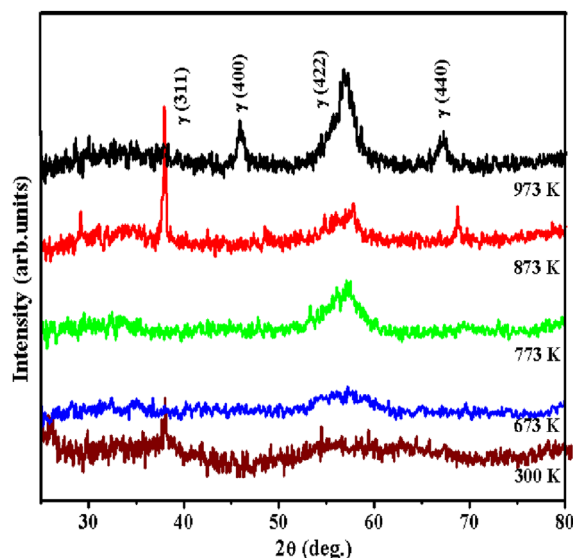


Fig. 1. XRD pattern of the  $\text{Al}_2\text{O}_3$  films prepared at various substrate temperatures at an oxygen partial pressure of  $3 \times 10^{-3}$  mbar.

coatings [19]. The anti-reflection coatings are commonly used in instrument panels, displays, camera lenses, binoculars and telescopes to help produce clear and sharper images and all these applications require smooth films with stoichiometry and low defects density. It is well known that the properties are dependent on the preparation method and processing parameters. Hence it is important to investigate the correlation among the process parameters, microstructure and properties for several technological applications.

$\text{Al}_2\text{O}_3$  exhibits different crystallographic polymorphs such as  $\gamma$ ,  $\eta$ ,  $\theta$ ,  $\delta$  and  $\alpha$  phases with respect to temperature. Among the different phases of  $\text{Al}_2\text{O}_3$ ,  $\gamma$  phase occurs in low temperature and find several technological applications [20].  $\text{Al}_2\text{O}_3$  thin films are deposited by different methods [21–25]. Among these methods, the pulsed laser deposition (PLD) is very flexible, simple, free from contamination, fast and controllable method for making high quality thin films of metals, semiconductors, insulators, polymers and biological materials. There are several reports on the preparation of  $\text{Al}_2\text{O}_3$  thin films by PLD. However, there is no systematic study on microstructural, optical and mechanical properties of  $\gamma\text{-Al}_2\text{O}_3$  films prepared as a function of substrate temperature. Hence, the present investigation deals with the preparation of  $\text{Al}_2\text{O}_3$  thin films on Si (100) and quartz substrates as a function of substrate temperature (300–973 K) in order to understand the influence of substrate temperature on the microstructure, optical and mechanical properties of the films.

## 2. Experimental details

$\text{Al}_2\text{O}_3$  (99.99% purity) powder was compacted into a pellet of 25 mm diameter and 3 mm thickness at a pressure of 10 MPa using a uni-axial press. The pellet was sintered at 1473 K for 6 h. PLD experiments were performed using a KrF excimer laser ( $\lambda=248$  nm) and the other deposition parameters are given elsewhere [23]. The thickness of the films was

measured by Dektak profilometer (DEKTAK 6M-stylus profiler). The crystallinity of films were studied in an INEL XRG-3000 X-ray diffractometer (GIXRD) using  $\text{CuK}\alpha_1$  radiation. HRTEM investigations were carried out on a JEOL 2000 EX II (T) operated at 200 kV. The surface morphology and root mean square (RMS) surface roughness of the films were examined by Nanoscope E (Digital instruments Inc., Model: NSE, USA) atomic force microscope (AFM) in contact mode. The optical properties were measured by a SOPRA ESGV model rotating polarizer ellipsometer in the energy range 1.5–5.5 eV for three different angles of incidence ( $65^\circ$ ,  $70^\circ$  and  $75^\circ$ ). The optical properties were also measured by a UV–vis–NIR (model no:3101/PC, Shimadzu) spectrophotometer in the wavelength range 190–800 nm. The mechanical measurements were carried out by nanoindenter (CSM, Switzerland) equipped with a Berkovich diamond indenter tip.

## 3. Results and discussion

### 3.1. Microstructural characterization

#### 3.1.1. XRD, TEM and AFM analysis

The sintered  $\text{Al}_2\text{O}_3$  pellet ( $\alpha\text{-Al}_2\text{O}_3$  of hexagonal structure,  $a=4.75$  Å, and  $c=12.99$  Å) was used as a target for PLD [23].  $\text{Al}_2\text{O}_3$  thin films were deposited on Si (100) and quartz substrates by PLD in the substrate temperatures range 300–973 K. Fig. 1 shows the XRD pattern of the  $\text{Al}_2\text{O}_3$  films and revealed that the films were amorphous at low substrate temperatures (300–673 K), and polycrystalline  $\text{Al}_2\text{O}_3$  in the temperatures  $\geq 773$  K. The films deposited in the temperatures  $\geq 773$  K indicated (311), (400), (422) and (440) reflections, correspond to  $\gamma\text{-Al}_2\text{O}_3$  of face centered cubic structure [26,27]. The peak intensities of the films increased with increasing substrate temperatures. The mean crystallite size was determined from the Scherrer formula after subtracting the instrumental broadening. The crystallite size was found to increase from 5 to 10 nm as the temperature increased from 300 K to 973 K. The phase formation depends on the preparation method and process parameters. In general, phase formation of  $\text{Al}_2\text{O}_3$  depends strongly on the substrate temperature [28]. It was reported by Cibert et al. [24] that the films prepared by plasma enhanced chemical vapor deposition (PECVD) at room temperature were amorphous, whereas the films showed cubic  $\gamma\text{-Al}_2\text{O}_3$  structure at 1073 K. Also, the  $\gamma\text{-Al}_2\text{O}_3$  films prepared by the PLD technique were reported to be formed at a substrate temperature of 1063 K only [29]. Pradhan et al. [30] have deposited  $\text{Al}_2\text{O}_3$  thin films by metal organic chemical vapor deposition as a function of temperature. The films were amorphous at the low temperature range 623–823 K and crystalline  $\text{Al}_2\text{O}_3$  phase in the temperature range 823–1023 K. Zywitzki et al. [22] have reported the nanocrystalline  $\gamma\text{-Al}_2\text{O}_3$  layers with a grain size of 12–15 nm at a substrate temperature of 973 K. Anders et al. [31] reported the  $\alpha$ -phase  $\text{Al}_2\text{O}_3$  by post-annealing at 1273 K for 16 h. In the present work,  $\gamma\text{-Al}_2\text{O}_3$  films were obtained at a low substrate temperature of 773 K due to the optimized oxygen partial pressure

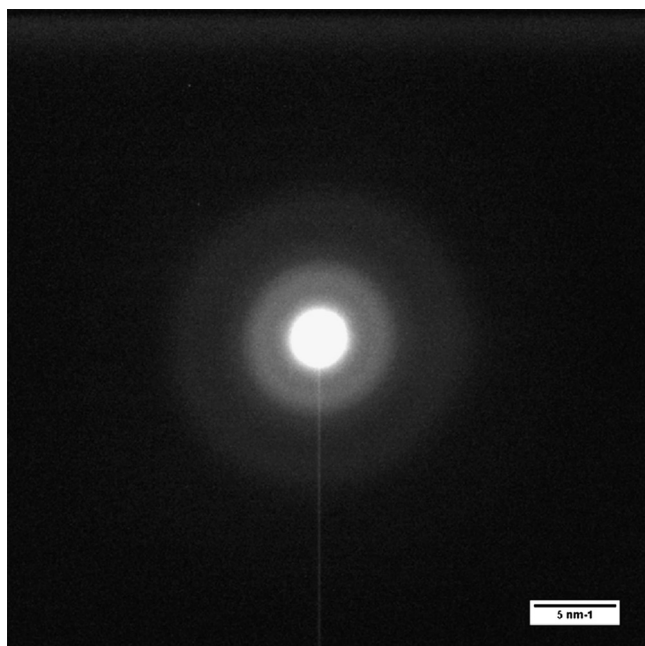


Fig. 2. SAED pattern of the  $\text{Al}_2\text{O}_3$  film. The diffuse ring pattern indicates the amorphous nature of alumina.

( $3.0 \times 10^{-3}$  mbar) and higher energy ( $\sim 30$ – $100$  eV) possessed by the ablated species produced from the target.

The  $\text{Al}_2\text{O}_3$  film was also deposited on NaCl single crystal at 673 K in an optimized oxygen partial pressure of  $3 \times 10^{-3}$  mbar. The as-deposited film on NaCl single crystal was immersed in distilled water and the film floated on the surface was transferred to 3 mm Cu grid. The structure of the  $\text{Al}_2\text{O}_3$  film was investigated by TEM. Fig. 2 shows the selected area of electron diffraction (SAED) pattern of the film. The diffraction pattern showed a diffuse ring pattern indicating the amorphous nature of the film. Hence, the TEM analysis confirmed the formation of amorphous  $\text{Al}_2\text{O}_3$  film at a substrate temperature of 673 K and the result is in agreement with XRD results.

The surface morphology of the films was analyzed by AFM. Fig. 3(a–d) shows the surface morphology of the films deposited at (a) 300 K, (b) 773 K, (c) 873 K and (d) 973 K. The film indicated a few crystallites at room temperature due to very low nucleation rate and the crystallites were more at 973 K. As a consequence the RMS roughness was found to be 0.3 nm at 300 K, 0.9 nm at 773 K and 2.3 nm at 973 K. Fig. 4 shows that the surface roughness increased with increasing substrate temperature. The increase in atomic mobility with increasing substrate temperature, enables thermodynamically favored grains to grow, resulting in increase of surface roughness [32,33].

### 3.2. Optical characterization

#### 3.2.1. Spectroscopic ellipsometer

The changes in amplitude ( $\tan \psi$ ) and phase difference ( $\cos \Delta$ ) between the parallel ( $r_p$ ) and perpendicular ( $r_s$ ) components of the reflected light polarized with respect to the plane of incidence are measured from the ellipsometry.

The optical pseudo-dielectric function,  $\epsilon(E)$ , was deduced from the ellipsometric parameters ( $\tan \psi$  and  $\cos \Delta$ ) [23,34]. The real and imaginary parts of the pseudo-dielectric functions  $\epsilon_1$  and  $\epsilon_2$  were computed from the experimentally measured ellipsometric parameters for the films prepared at different substrate temperatures. A three phase model (ambient/ $\text{Al}_2\text{O}_3$ /c-Si) was assumed to evaluate the thickness and refractive indices of the films. A linear regression analysis was carried out, until the mean square deviation ( $\chi^2$ ) between computed and experimental values was less than  $\sim 10^{-3}$ . To improve the quality of fit, roughness was taken into consideration. Hence, the four phase model (substrate/ $\text{Al}_2\text{O}_3$ /roughness/ambient) [35] was used to estimate the surface roughness, which was assumed to be a mixture of  $\text{Al}_2\text{O}_3$  and voids on the basis of Bruggemen effective medium approximation (BEMA) [36]. The experimental and calculated ellipsometric parameters ( $\tan \psi$  and  $\cos \Delta$ ) of a representative film prepared at 773 K are shown in Fig. 5(a, b). The thickness and refractive indices of films were extracted from BEMA model and given in the present work. The complex refractive index,  $N$  ( $N=n+ik$ ) of the films was extracted using a Cauchy dispersion model given by

$$N(\lambda) = A + (B/\lambda^2) + (C/\lambda^4)$$

where  $n$  is the refractive index;  $k$  is the absorption;  $A$ ,  $B$  and  $C$  are the Cauchy parameters; and  $\lambda$  is the incident wavelength. The  $A$  parameter is very dominant compared to  $B$  and  $C$  parameters. That is why, only  $A$  parameter is reported in Table 1. The typical values of  $B$  and  $C$  in our case are  $\sim 1.9 \times 10^{-3}$  and  $2.8 \times 10^{-4}$  respectively. Fig. 6 shows the variation of refractive index as a function of photon energy. The refractive indices were found to increase from 1.698 to 1.749 (at 632.8 nm) as the temperature increased from 300 K to 973 K. For all the films, the refractive indices increased with increasing photon energy. The refractive indices of the films increased with increasing substrate temperature and in accordance with the trends reported in the literature [37,38]. At higher substrate temperatures, the adatom mobility is higher compared to those at low substrate temperatures. The higher mobility causes formation of films with increased crystallite size, reduced porosity and defects. These beneficial factors could produce films of higher packing density and hence its refractive index. No absorption ( $k=0$ ) was observed in all the films deposited at different substrate temperatures.

#### 3.2.2. UV-visible spectrophotometer

The transmittance of  $\text{Al}_2\text{O}_3$  films was measured over the range 190–800 nm wavelength using UV-visible spectrophotometer. The transmittance spectra of  $\text{Al}_2\text{O}_3$  films deposited at different temperatures are shown in Fig. 7. The oscillations in the spectra indicating the interference of light between the film and substrate. The UV-visible spectroscopy studies showed that all the films had transmittance  $> 80\%$ . The refractive indices were calculated using the



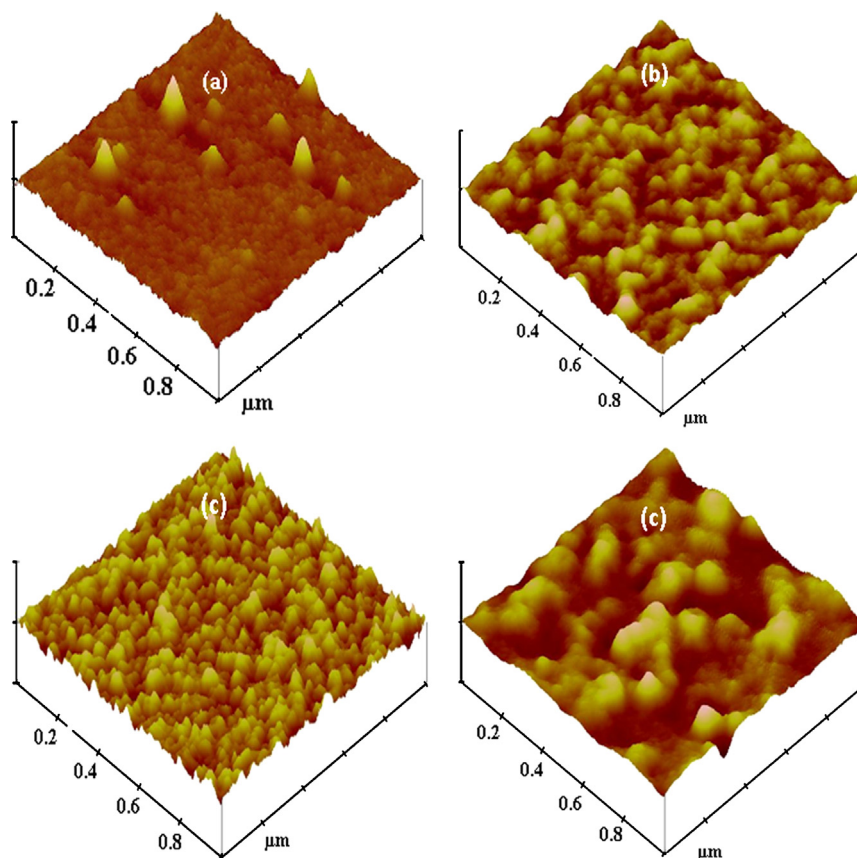


Fig. 3. AFM images ( $1 \times 1 \mu\text{m}^2$ ) of the  $\text{Al}_2\text{O}_3$  thin films deposited at (a) 300 K, (b) 773 K, (c) 873 K and (d) 973 K.

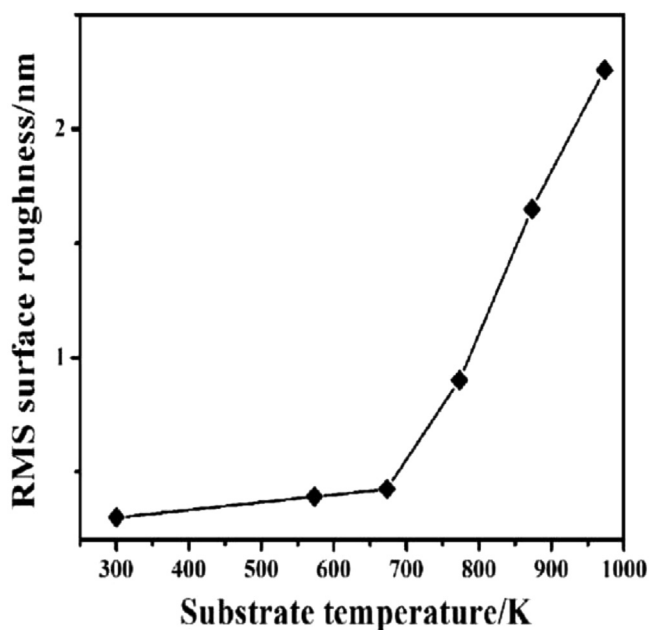


Fig. 4. The plot of RMS roughness of the  $\text{Al}_2\text{O}_3$  films versus substrate temperature.

transmittance spectra [33,39]. The study showed that the refractive indices increased from 1.65 to 1.80 (at 632.8 nm) as the temperature increased from 300 K to 973 K [24]. The

refractive indices of the films increased with increasing substrate temperature (Fig. 7 inset) [32,33]. The increase in refractive indices could be due to an increase of films density. The extinction coefficients ( $k$ ) for the films were calculated and found to be 0.0165 and 0.00484 for the films deposited at 300 K and 773 K, respectively and then the  $k$  value decreased to 0.0044 at 973 K. Thus, it was found that the extinction coefficient decreased with increasing substrate temperature. There are several reports on the influence of deposition temperature on the refractive indices of the films. Lin et al. [17] deposited  $\text{Al}_2\text{O}_3$  thin films on glass and silicon substrates by RF plasma enhanced chemical vapor deposition and refractive index of 1.61–1.73 was obtained. Koski et al. [40] measured the refractive indices and found to be in the range 1.52–1.83 with a hardness of 7–12 GPa [41,42]. Amorphous  $\text{Al}_2\text{O}_3$  films were prepared on glass and silicon substrates by low-pressure metal-organic chemical vapor deposition and showed refractive index values in the range 1.60–1.74 [43].  $\text{Al}_2\text{O}_3$  thin films were deposited on Si (100) by spray pyrolysis in the substrate temperature range 723–923 K and found the refractive index of 1.66 (at 630 nm) from the ellipsometric measurements.  $\text{Al}_2\text{O}_3$  films were produced by oxygen-ion assisted deposition as a function of substrate temperature (300–573 K). The as-deposited films were amorphous and the maximum refractive index of 1.73 was obtained for the film deposited at 573 K. The films deposited at elevated substrate temperatures were more

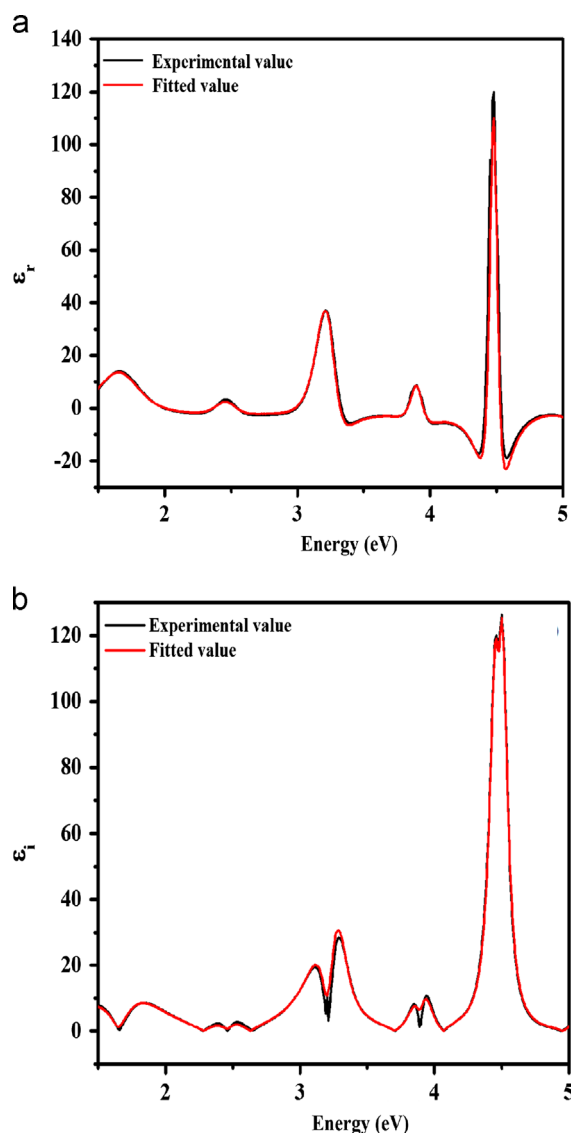


Fig. 5. Experimental and fitted ellipsometric parameters for a representative  $\text{Al}_2\text{O}_3$  film deposited at 773 K, (a) real part of dielectric function versus photon energy and (b) imaginary part of the dielectric function versus photon energy.

Table 1

Ellipsometry measurements of thickness and refractive index of the  $\text{Al}_2\text{O}_3$  films.

Temperature (K)	A parameter	Thickness (nm)	Refractive index @ 632.8 nm Ellipsometer
300	1.66	270	1.698
673	1.67	269	1.718
773	1.72	258	1.735
873	1.73	279	1.749
973	1.74	260	1.749

stable with high refractive index and low extinction coefficient [44]. In the present work, the refractive indices and extinction coefficients values obtained from both ellipsometry and UV–visible studies are nearly same. Therefore, it is clear that the variation in the refractive indices quoted in the literature and in

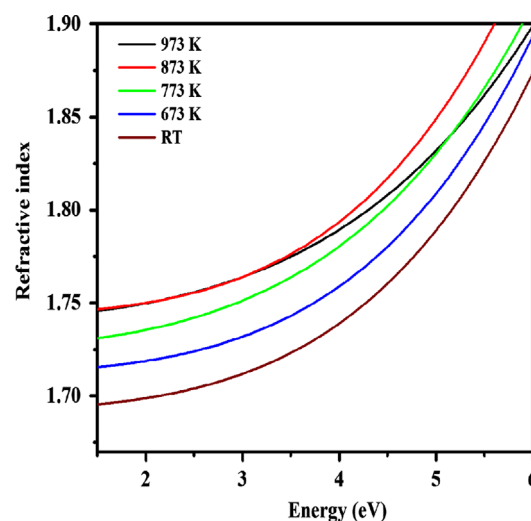


Fig. 6. Refractive index versus photon energy (eV) of the  $\text{Al}_2\text{O}_3$  films deposited at different substrate temperatures.

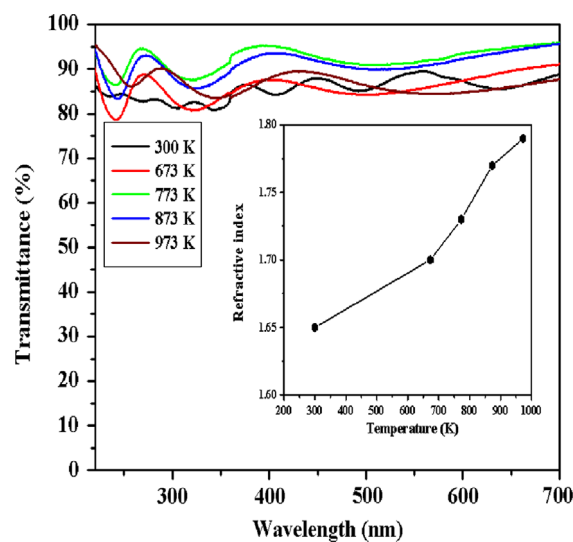


Fig. 7. Transmittance versus wavelength of the deposited films on quartz substrate at various temperatures. Inset shows the refractive index (at 632.8 nm) versus substrate temperature.

the present work is due to the differences in the microstructure of the films prepared by the different deposition methods and process parameters [3,6,9,11].

### 3.3. Nanoindentation studies

Nanoindentation measurements were carried out to find the hardness and elastic modulus of  $\text{Al}_2\text{O}_3$  films ( $\sim 1 \mu\text{m}$  thickness) deposited at 300 K and 973 K temperatures. Fig. 8 shows the typical load-depth curve for finding the hardness and Young's modulus of the film prepared at 973 K. The hardness of the  $\gamma\text{-Al}_2\text{O}_3$  films was found to be 20.8 GPa and 24.7 GPa for the films deposited at 300 and 973 K respectively. The elastic modulus of the films were found to be 320 and 360 GPa for the above temperatures [40–42]. The increased hardness of the films could be correlated with higher deposition temperature (higher

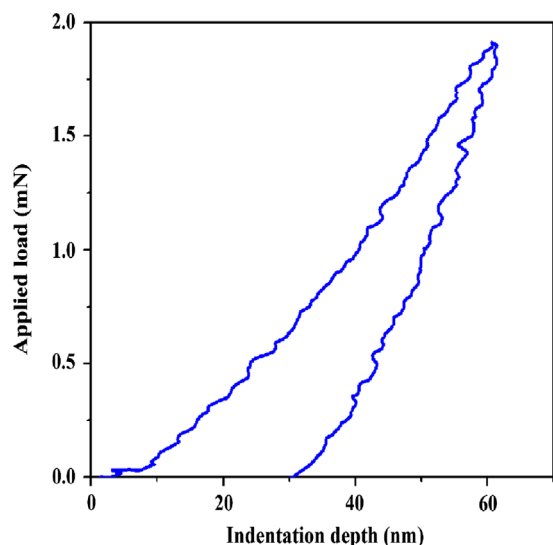


Fig. 8. Load versus indentation depth curve of  $\gamma$ - $\text{Al}_2\text{O}_3$  film prepared at 973 K.

mobility of ad-atoms) causes higher packing density of the films. Schutze et al. [45] deposited 2  $\mu\text{m}$   $\gamma$ - $\text{Al}_2\text{O}_3$  film by reactive sputtering and nanoindentation studies showed the hardness and elastic modulus of  $\sim 25$  GPa and 350 GPa respectively. Zhao et al. [46] deposited the  $\text{Al}_2\text{O}_3$  films on Si (100) and quartz substrates at 673 K by filtered cathodic vacuum arc system and found the hardness of 7.6 GPa. The refractive index and hardness of the films increased with substrate temperature at optimized conditions, which makes films for potential applications in optical, hard and wear-resistant coatings [8,11]. Therefore, the microstructural factors play a decisive role in influencing the optical and mechanical properties of the films [3,6,9,11].

#### 4. Conclusions

The  $\text{Al}_2\text{O}_3$  films were deposited on Si (100) and quartz substrates in the substrate temperature range 300–973 K by PLD. The XRD studies indicated the amorphous nature of the films at low substrate temperatures (300–673 K) and cubic  $\gamma$ - $\text{Al}_2\text{O}_3$  phase at higher substrate temperatures ( $\geq 773$  K). The TEM investigation confirmed the amorphous nature of the  $\text{Al}_2\text{O}_3$  film prepared at a substrate temperature of 673 K. The AFM investigation showed the smooth morphology of the films and RMS surface roughness increased from 0.3 to 2.3 nm with increasing substrate temperature. The ellipsometry and UV–visible spectroscopy analysis revealed that the refractive index values increased from 1.698 to 1.749 and 1.65 to 1.80 (at 632.8 nm), respectively as the temperature increased from 300 to 973 K. The hardness values of 20.8 GPa and 24.7 GPa were obtained for the amorphous (300 K) and  $\gamma$ - $\text{Al}_2\text{O}_3$  films (973 K), respectively. The variation in the optical and mechanical properties is correlated with the changes in the microstructural features of the films prepared as a function of substrate temperature.

#### Acknowledgments

The authors would like to thank Dr. M. Vijayalakshmi, AD, Physical Metallurgy Group, Dr. T. Jayakumar, Director, Metallurgy and Materials Group and Shri S.C. Chetal, Director, IGCAR, Kalpakkam for their encouragement and support. The authors (J.I.S. and G.B.) are thankful for the National Research Foundation of Korea (NRF) Grant funded by the Korea Government (MEST) under the Grant no. 2012-0009455.

#### References

- [1] R.F. Bunshah, Handbook of Hard Coatings, Noyes Publications, New Jersey, 2001.
- [2] S.-S. Lin, Effect of fibered morphology on the properties of  $\text{Al}_2\text{O}_3$  nanoceramic films, Ceramics International 39 (2013) 3157–3163.
- [3] D.H. Kuo, B.Y. Cheung, R.J. Wu, Growth and properties of alumina films obtained by low-pressure metal-organic chemical vapor deposition, Thin Solid Films 398–399 (2001) 35–40.
- [4] M. Aguilar-Frutos, M. Garcia, C. Falcony, Optical and electrical properties of aluminum oxide films deposited by spray pyrolysis, Applied Physics Letters 72 (1998) 1700–1702.
- [5] C.H. Lin, H.L. Wang, M.H. Hon, The effect of residual stress on the adhesion of PECVD-coated aluminum oxide film on glass, Thin Solid Films 283 (1996) 171–174.
- [6] M. Hiratani, K. Torii, Y. Shimamoto, S.I. Saito, Built-in interface in high- $\kappa$  gate stacks, Applied Surface Science 216 (2003) 208–214.
- [7] S. Prasanna, G. Mohan Rao, S. Jayakumar, M.D. Kannan, V. Ganesan, Dielectric properties of DC reactive magnetron sputtered  $\text{Al}_2\text{O}_3$  thin films, Thin Solid Films 520 (2012) 2689–2694.
- [8] H.L. Wang, C.H. Lin, M.H. Hon, The dependence of hardness on the density of amorphous alumina thin films by PECVD, Thin Solid Films 310 (1997) 260–264.
- [9] N. Ozer, J.P. Cronin, Y.J. Yao, A.P. Tomsia, Optical properties of sol-gel deposited  $\text{Al}_2\text{O}_3$  films, Solar Energy Materials and Solar Cells 59 (1999) 355–366.
- [10] J. Park, Y.Y. Noh, J.W. Huh, J. Lee, H. Chu, Optical and barrier properties of thin-film encapsulations for transparent OLEDs, Organic Electronics 13 (2012) 1956–1961.
- [11] J. Wanga, Y.H. Yub, S.C. Leeb, Y.W. Chung, Tribological and optical properties of crystalline and amorphous alumina thin films grown by low-temperature reactive magnetron sputter-deposition, Surface and Coatings Technology 146–147 (2001) 189–194.
- [12] K. Tadanaga, J. Morinaga, A. Matsuda, T. Minami, Superhydrophobic-superhydrophilic micropatterning on flowerlike alumina coating film by the sol-gel method, Chemistry of Materials 12 (3) (2000) 590–592.
- [13] J.W. Lee, C.W. Won, B.S. Chun, H.Y. Sohn, Dip coating of alumina films by the sol-gel method, Journal of Materials Research 8 (1993) 3151–3157.
- [14] G. Yi, M. Sayer, Sol-gel processing of complex oxide films, Ceramic Bulletin 70 (1991) 1173–1179.
- [15] C.M. Chiang, L.S. Chang, Microstructure and characterization of aluminum oxide thin films prepared by reactive RF magnetron sputtering on copper, Surface and Coatings Technology 198 (2005) 152–155.
- [16] C.H. Lin, H.L. Wang, M.H. Hon, Preparation and characterization of aluminum oxide films by plasma enhanced chemical vapor deposition, Surface and Coatings Technology 90 (1997) 102–106.
- [17] B. Behkam, Y. Yang, M. Asheghi, Thermal property measurement of thin aluminum oxide layers for giant magnetoresistive application, International Journal of Heat and Mass Transfer 48 (2005) 2023–2031.
- [18] W. Zhang, W. Liu, C. Wang, Effects of solvents on the tribological behaviour of sol-gel  $\text{Al}_2\text{O}_3$  films, Ceramics International 29 (2003) 427–434.
- [19] A.W. Adamson, Physical Chemistry of Surfaces, 5th ed., Wiley, New York, 1990.

- [20] Y. Wang, J. Wang, M. Shen, W. Wang, Synthesis and properties of thermostable  $\gamma$ -alumina prepared by hydrolysis of phosphide aluminum, *Journal of Alloys and Compounds* 467 (2009) 405–412.
- [21] K.S. Shamala, L.C.S. Murthy, K. Narasimha Rao, Studies on optical and dielectric properties of  $\text{Al}_2\text{O}_3$  thin films prepared by electron beam evaporation and spray pyrolysis method, *Materials Science and Engineering B* 106 (2004) 269–274.
- [22] O. Zywitzki, K. Goedicke, H. Morgner, Structure and properties of  $\text{Al}_2\text{O}_3$  layers deposited by plasma activated electron beam evaporation, *Surface and Coatings Technology* 151–152 (2002) 14–20.
- [23] G. Balakrishnan, P. Kuppusami, S. Tripura Sundari, R. Thirumurugesan, V. Ganesan, E. Mohandas, D. Sastikumar, Structural and optical properties of  $\gamma$ -alumina thin films prepared by pulsed laser deposition, *Thin Solid Films* 518 (2010) 3898–3902.
- [24] C. Cibert, H. Hidalgo, C. Champeaux, P. Tristant, C. Tixier, J. Desmaison, A. Catherinot, Properties of aluminum oxide thin films deposited by pulsed laser deposition and plasma enhanced chemical vapor deposition, *Thin Solid Films* 516 (2008) 1290–1296.
- [25] A. Pillonnet, C. Garapon, C. Champeaux, C. Bovier, R. Bregnier, H. Jaffrezic, J. Mugnier, Influence of oxygen pressure on structural, optical properties of  $\text{Al}_2\text{O}_3$  optical waveguides prepared by pulsed laser deposition, *Applied Physics A: Materials and Processing* 69 (1999) S735–S738.
- [26] J. Gottmann, E.W. Kreutz, Pulsed laser deposition of alumina and zirconia thin films on polymers and glass as optical and protective coatings, *Surface and Coatings Technology* 116–119 (1999) 1189–1194.
- [27] K.R. Murali, P. Thirumoorthy, Characteristics of sol–gel deposited alumina films, *Journal of Alloys and Compounds* 500 (2010) 93–95.
- [28] C.H. Peng, C.C. Hwang, C.S. Hsiao, Structure and photoluminescence properties of strong blue-emitting alumina film developed from a liquid sol at low temperature, *Journal of Alloys and Compounds* 491 (2010) L29–L32.
- [29] B.K. Tay, Z.W. Zhao, D.H.C. Chua, Review of metal oxide films deposited by filtered cathodic vacuum arc technique, *Materials Science and Engineering R* 52 (2006) 1–48.
- [30] S.K. Pradhan, Philip J. Reucroft, Yeonkyu. Ko, Crystallinity of  $\text{Al}_2\text{O}_3$  films deposited by metalorganic chemical vapor deposition, *Surface and Coatings Technology* 176 (2004) 382–384.
- [31] S. Anders, A. Anders, M. Rubin, Z. Wang, S. Raoux, F. Kong, I. G. Brown, Formation of metal oxides by cathodic arc deposition, *Surface and Coatings Technology* 76–77 (1995) 167–173.
- [32] G. Balakrishnan, S. Tripura Sundari, P. Kuppusami, P. Chandra Mohan, M.P. Srinivasan, E. Mohandas, V. Ganesan, D. Sastikumar, A study of microstructural and optical properties of nanocrystalline ceria thin films prepared by pulsed laser deposition, *Thin Solid Films* 519 (2011) 2520–2526.
- [33] G. Balakrishnan, K. Thanigaiaarul, P. Sudhakara, Jung Il Song, Microstructural and optical properties of nanocrystalline undoped zirconia thin films prepared by pulsed laser deposition, *Applied Physics A: Materials Science and Processing* 110 (2013) 427–432.
- [34] R.M.A. Azzam, N.M. Bashara, *Ellipsometry and Polarized light*, North-Holland, Amsterdam, 1988.
- [35] E.D. Palik (Ed.), *Hand Book of Optical Constants of Solids*, vol. II, Academic Press, 1998.
- [36] M. Eрман, J.B. Theeten, P. Chambon, S.M. Kelso, D.E. Aspnes, Optical properties and damage analysis of GaAs single crystals partly amorphized by ion implantation, *Journal of Applied Physics* 56 (1984) 2664–2671.
- [37] C.C. Lee, D.T. Wei, J.C. Hsu, C.H. Shen, Influence of oxygen on some oxide films prepared by ion beam sputter deposition, *Thin Solid Films* 290–291 (1996) 88–93.
- [38] Z.W. Zhao, B.K. Tay, L. Huang, S.P. Lau, J.X. Gao, Influence of thermal annealing on optical properties and structure of aluminum oxide thin films by filtered cathodic vacuum arc, *Optical Materials* 27 (2004) 465–469.
- [39] G. Balakrishnan, T.N. Sairam, P. Kuppusami, R. Thirumurugesan, E. Mohandas, V. Ganesan, D. Sastikumar, Influence of oxygen partial pressure on the properties of pulsed laser deposited nanocrystalline zirconia thin films, *Applied Surface Science* 257 (2011) 8506–8510.
- [40] K. Koski, J. Holsa, P. Juliet, Properties of aluminum oxide thin films deposited by reactive magnetron sputtering, *Thin Solid Films* 339 (1999) 240–248.
- [41] J.M. Schneider, W.D. Sproul, R.W.J. Chia, M.S. Wong, A. Matthews, Very-high-rate reactive sputtering of alumina hard coatings, *Surface and Coatings Technology* 96 (1997) 262–266.
- [42] F. Fietzke, K. Goedicke, W. Hempel, The deposition of hard crystalline  $\text{Al}_2\text{O}_3$  layers by means of bipolar pulsed magnetron sputtering, *Surface and Coatings Technology* 86–87 (1996) 657–663.
- [43] M. Aguilar-Frutos, M. Garcia, C. Falcony, G. Plesch, S. Jimenez-Sandoval, A study of the dielectric characteristics of aluminum oxide thin films deposited by spray pyrolysis from  $\text{Al}(\text{acac})_3$ , *Thin Solid Films* 389 (2001) 200–206.
- [44] M.S. Al-Robaee, G.N. Subbanna, K. Narasimha Rao, S. Mohan, Studies of the optical and structural properties of ion-assisted deposited  $\text{Al}_2\text{O}_3$  thin films, *Vacuum* 45 (1994) 97–102.
- [45] A. Schutze, D.T. Quinto, Pulsed plasma-assisted PVD sputter-deposited alumina thin films, *Surface and Coatings Technology* 162 (2003) 174–182.
- [46] Z.W. Zhao, B.K. Tay, D. Sheeja, Structural characteristics and mechanical properties of aluminum oxide thin films prepared by off-plane filtered cathodic vacuum arc system, *Surface and Coatings Technology* 167 (2003) 234–239.